Journal of Geodynamics 127 (2019) 42–51

Contents lists available at ScienceDirect

Journal of Geodynamics

journal homepage: www.elsevier.com/locate/jog

Seismo ionospheric anomalies before the 2007 M7.7 Chile earthquake from GPS TEC and DEMETER

Munawar Shah[a,*], M. Arslan Tariq[b], Junaid Ahmad[b], Najam Abbas Naqvi[a], Shuanggen Jin[c]

[a] Institute of Space Technology, Islamabad 44000, Pakistan
[b] Centre for Earthquake Studies, National Centre for Physics, Islamabad, Pakistan
[c] Shanghai Astronomical Observatory, Shanghai, China

ARTICLE INFO

Keywords:
Seismo ionospheric anomalies
DEMETER
GPS
TEC
ISL

ABSTRACT

Earthquake (EQ) related variations in the ionosphere may provide some insights to understand the seismo ionospheric coupling and to mitigate the damages of seismic hazards. In this paper, the electromagnetic variations in the ionosphere associated with November 14, 2007, M7.7 Chile EQ are investigated in electron density and electron temperature measurements from ISL (Langmuir Probe) of DEMETER (Detection of Electro-Magnetic Emissions Transmitted from Earthquake Regions) satellite and TEC (total electron content) estimated from GPS (Global Positioning System). The investigation of temporal and spatial measurements suggests anomalies which are observed within 10 days before the future EQ (i.e. 9 days before on November 5, 2007). The temporal values of daytime DEMETER and diurnal TEC on November 5, 2007 imply abrupt anomalies that are considered to be the fragments of the plasma intensification process in the Southern Hemisphere activated by the rock compression in the quake region. Similarly, spatial maps of TEC and DEMETER (electron density and electron temperature) showed the anomalous configuration of the temporal analysis that may induce by the epicenter. In addition to spatial and temporal analysis, the Index number for the northern and southern sectors of the EQ preparation zone around the epicenter along latitude confirmed the anomalous values of electron density and electron temperature of the DEMETER satellite. Similarly, the comparison of electron density and electron temperature at the epicenter latitude and its conjugate reveals anomalous enhancement over the seismogenic zone on November 5, 2007 (9 days before) prior to the event.

1. Introduction

The association of EQ and ionospheric precursors has been widely reported from the analysis of GPS TEC (Liu et al., 2004; Liu et al., 2006; Heki and Enomoto, 2013; Shah and Jin, 2015; Arslan et al., 2019), satellite-based electron density and on the underlying mechanism of EQ precursor between the ground to atmosphere interface (Oyama et al., 2008; Oyama et al., 2011; Li and Parrot, 2012; Ryu et al., 2014). However, there is still an uncertainty in the EQ anomalies reports due to lack of unified, indisputable and explicit definition, how they generated and why they spread before and after the EQ over the seismogenic zones. For example, there are some reports against the existence of EQ precursors (Geller et al., 1997; Rishbeth, 2007); some even strongly stated that EQ prediction is complicated with the existed precursor's equipment. Meanwhile, the progress in statistical analyses on GPS TEC (Shah and Jin, 2015) and satellite data (Li and Parrot, 2012) suggested an undisputed connection between the EQs and existence of the ionospheric anomalies occurred in the ionosphere.

In a report, Ryu et al. (2014) calculated the ratio of the equatorial electron density to the mid-latitude electron density and observed EQ intensified EIA (equatorial ionization anomaly) before March 2005 (M8.7 Northern Sumatra) and the M8.0 Pisco EQ in August 2007. They suggested that some of the large equatorial EQs can cause a significant enhancement in the electron density and temperature at the geomagnetic equator and mid-latitude regions. Similarly, Shah and Jin (2015) statistically proved the existence of ionospheric anomalies before large magnitude EQs within the preparation zone. It means that during the EQ preparation period, there exists some unusual ionospheric behavior over the seismogenic zone.

Based on the method of detection in previous reports of EQ precursors, the seismically induced precursors can be of many classes (i.e., plasma waves, both ionic and electron density of plasma and temperature, infrared radiation (IR), and energetic particles). Following these precursor procedures, Larkina et al. (1989) detected significant

* Corresponding author.
E-mail addresses: munawar.shah@mail.ist.edu.pk, shahmunawar1@gmail.com (M. Shah).

https://doi.org/10.1016/j.jog.2019.05.004
Received 22 August 2018; Received in revised form 10 May 2019; Accepted 18 May 2019
Available online 20 May 2019

enhancement in the intensity of low-frequency (0.1-1.6 kHz) radio wave emissions found in the measurements of INTERCOSMOS-19 data when the satellite crossed over the epicenter of the future EQ. In their statistical observation for different EQs, they pointed out that the enhancement of ELF/VLF emissions occurs between tens of minutes and hours before/after the events.

The deviations in the observations from experimental data were recorded in the form of enhancement before a number of large magnitude EQs (Gokhberg et al., 1989). Later on, a theoretical study was followed to explain the physical existence of anomalous ELF/VLF emissions over the seismogenic zones (Sorokin et al., 1998). According to Sorokin et al. (2003), a scaled abnormality from the low-altitude atmosphere above the seismogenic zone can start transient abnormalities of the plasma and electromagnetic field due to vertical, turbulent exchange of charge aerosols and radioactive particles. Subsequently, the interaction between the short-term abnormalities in conductivity with the electromagnetic radiation results in ELF emissions in the upper atmosphere and ULF fluctuations at the Earth's surface.

On the other hand, Bošková et al. (1993) found a significant enhancement in the data of light ions in the ionosphere specifically, H + and He + retrieved by the low orbit INTERCOSMOS-24 satellite. Similarly, Chmyrev et al. (1997) reported ionospheric irregularities in the ELF emissions, plasma density Ne and differential dNe data of the COSMOS-1809 satellite over the epicenter of the Spitak EQ event. They studied that ELF waves possessed irregularities in plasma (˜ dNe/Ne = 38%) at a distance of 4-10 km along the orbit, which was formed beside the geomagnetic flux tubes linked to the EQ breed zone.

Shklyar and Truhlík (1998) investigated the formation and role of a quasi-static transverse electric field in altering the plasma density distribution and discussed different arguments for the mechanism of modifying the ion concentration profiles connected with radioactive emanation prior to the main shock. Hayakawa et al. (1993) reported a strong connection between the ion density irregularities in the ionosphere and global distribution of seismic events, based on a large scale data collected by the INTERCOSMOS-24 satellite. They found a clear correlation for daytime (10:00-16:00 LT) between EQ and plasma density, involving huge magnetic disturbance at altitudes of 500-700 km. However, these variations disappeared at night and during magnetic storms. Similarly, Oyama et al. (2008) reported an anomalous decrease in the electron density profiles of the HINOTORI satellite in the afternoon, before and after large EQs occurred during January 1982 in the Philippines. They attributed this significant fall in the electron temperature to the execution of electric fields over the epicenter of the future quakes. In the same sequence, Oyama et al. (2011) reported an anomalous reduction in the ion density data of US satellite DE-2 associated with M7.5. Electric fields generated around the epicenter of the future EQ are proposed to be the most credible candidates for the variations of the ionosphere at different altitudes.

There are several mechanisms existed for the generation of ionospheric anomalies over the epicenter and three of them got much attention. Among them, the stress activated positive-hole model (Freund, 2002), the model based on radon emanation (Ondoh, 2003), and the gravity waves atmospheric model (Namgaladze et al., 2009) got the attraction of the researchers in this field. Apart from this, the thermal infrared radiations (TIR) behaved abnormally over the fault lineaments of future EQ (Tronin, 1996). There were significant nighttime enhancements of the outgoing Earth radiation flux over the largest heterogeneous structures and fault systems in the seismogenic zone of the future EQ. This shows that integrated observations of ground and satellite instruments, with more theoretical support would certainly provide a unified, indisputable and explicit definitions of the seismo ionospheric anomalies. There also exist various approaches to study the seismo ionospheric anomalies. The notable methods are; the statistical seismo ionospheric analysis (Fujiwara et al., 2004; Liu et al., 2006; Shah and Jin, 2015; Junaid et al., 2018), case-study analysis (Oyama et al., 2008), and physical model analysis for explanation of ionospheric anomalies (Kuo et al., 2011; Namgaladze et al., 2009). The statistical approach is notable enough in proving that there actually have connections between the EQ and associated anomalies. On the other hand, the case studies and the physical model analyses are valid for showing the physical background of the existing seismo ionospheric anomalies. From the above explanations, seismic precursors are still controversial and there was no satellite mission for the detection of EQ associated ionospheric abnormalities before the DEMETER satellite (Parrot, 2002). DEMETER was a micro-satellite (130 kg mass) placed on a nearly polar orbit with a low altitude (710 km) providing a global coverage of active seismic regions (Cussac et al., 2006). According to Parrot (2009), the main scientific objectives of DEMETER include the variations in the ionosphere due to EQ induced electromagnetic activity and anthropogenic activities.

In this paper, we studied the ionospheric anomalies from GPS TEC maps over the epicenter of the future EQ (i.e. M7.7, Chile event). Similarly, the electron density and electron temperature measurements from the DEMETER are also studied to confirm the ionospheric abnormalities over the epicenter of M7.7 Chile EQ. The anomalies in electron temperature, electron density and total electron content explicitly followed the pattern of the EQ epicenter around the seismic preparation zone.

2. Data sources and method

The seismo ionospheric anomalies related to M7.7, Chile EQ are studied by considering the data from GPS TEC and DEMETER satellite over the epicenter. The Chile EQ of M7.7 on November 14, 2007, resulted from thrust faulting along the boundary between the oceanic Nazca plate and the South American continent, dubbed as the Antofagasta EQ (Fig. 1). In Fig. 1, one can see the EQ epicenter bounded by the EQ preparation zone and two flights of DEMETER on November

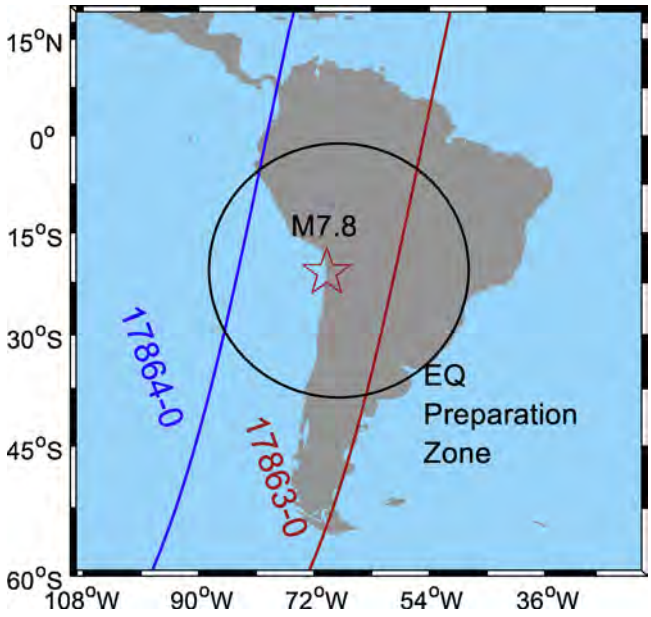

Fig. 1. Geographical position of M7.7 (Chile EQ) bounded by the two flights of DEMETER satellite (i.e. both the flights occurred on November 5, 2007 during daytime) before the main shock. The red star denotes the epicenter of the EQ, however the EQ preparation zone is marked by the black circle. (For interpretation of the references to colour in this figure legend, the reader is referred to the web version of this article).

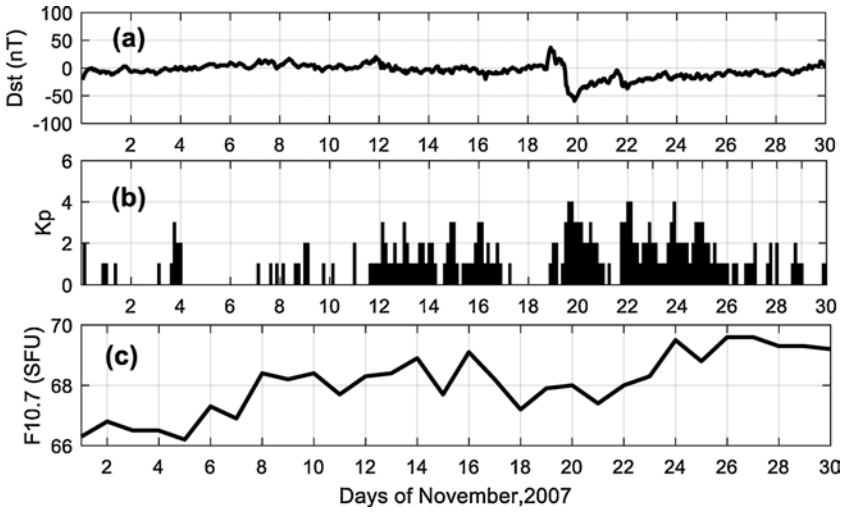

Fig. 2. Solar storm indices (Dst, Kp and F10.7) before and after the M7.7 (Chile) EQ. The indices are shown against the days of November, 2007. The EQ day is November 14, 2007.

5, 2007. It hits the southern coastal region of Chile (20.5 °S, 69.8 °W), at a shallow depth of 40 km. The main shock occurred at UT = 15:40 and was followed by many aftershocks along the South American arc. There are several reports about extensive precursory activity related to high magnitude EQ in the Chile region (Gusman et al., 2015; Ho et al., 2013; Píša et al., 2011; Yagi et al., 2014; Zhang et al., 2011).

The cause of this EQ is the moving of the Nazca plate towards the east-northeast at a velocity of 79 mm/year towards the South American continent (Survey, 2007b). The South American arc extends over 7000 km, from the Chilean margin triple junction offshore of southern Chile to its joint with the Panama fracture zone. Subduction begins at the Peru-Chile Trench, 85 km to the west of the huge M7.7 Chile EQ epicenter. To detect temporal and spatial ionospheric variations over the EQ breeding zone of the M7.7 Chile quake, the data of different ionospheric parameters were compiled from GPS and DEMETER. However, Altadill and Apostolov (2003) reported the geomagnetic anomalies in the ionosphere F2 layer, which were due to the extreme solar storm. Therefore, it is necessary to monitor the time and scale of the planetary solar-terrestrial indices before and after the strong EQ event to clearly spot the precise ionospheric precursor. For this purpose, geomagnetic storm indices of November 2007 were checked in the context of the M7.7 EQ (Fig. 2). The temporal series of the solar indices were obtained from the OMNI web NASA (National Aeronautics and Space Administration) and Kyoto University (http://wdc.kugi.kyoto-u.ac.jp/kp/Index.html).

To recognize the temporal and spatial anomalies, the daily TEC maps with two hour temporal resolution were retrieved from GIM-TEC (Global Ionospheric Map-Total Electron Content) over the EQ geographical epicenter. The GIM-TEC data was originally in the bi-hourly format; however, for the detection of anomalies, the TEC for 18 days before and 2 days after the main shock day is bounded by the confidence intervals. To identify any significant TEC anomalous trends, the daily TEC values are bounded by the confidence intervals of mean and standard deviation (Fig. 3a). The bounds are calculated by the mean and standard deviation of 15 days before and 5 days after the observed day using the below equation.

$$X_{\text{upper Bound}} = \mu + 2\sigma \quad (1)$$

$$X_{\text{lower Bound}} = \mu - 2\sigma \quad (2)$$

Similarly, the percentage deviations between the observed TEC and Upper/Lower bounds are found before and after the main shock, as shown in Fig. 3b.

$$\%\text{Deviation} = \begin{cases} \dfrac{OV - \text{Xhigh}}{Xhigh} \times 100 & OV > Xhigh \\ 0 & Xhigh \geq 0 \geq Xlower \\ \dfrac{OV - Xlower}{Xlower} \times 100 & OV < Xlower \end{cases} \quad (3)$$

In this paper, we used the electron density and electron temperature measurements from the ISL (Langmuir probe) instrument onboard the DEMETER satellite to confirm the EQ anomalies in daily TEC. DEMETER is a French micro-satellite dedicated to measuring the plasma parameters in the ionosphere over the most sensitive global seismogenic zones. DEMETER was operated at the orbit with an altitude of 710 km on June 24, 2004 and terminated officially on December 9, 2010 (Parrot et al., 2006). The satellite was initially launched at 710 km altitude in a sun-synchronous orbit with an ascending node crossing the local equatorial part at 22:00 LT (nighttime) and 10:30 LT (daytime). However, the altitude was then lowered to 660 km in December 2005 (Cussac et al., 2006). This enabled DEMETER to measure the ionospheric perturbations along both the hemispheres. DEMETER has two modes: (i) a survey mode to collect the whole earth data at latitude less than 65° and (ii) a burst mode to measure the data over the sensitive seismogenic zones. Further information about DEMETER satellite is available in (Berthelier et al., 2006; Ryu et al., 2014 and reference therein). We studied the daytime data from ascending flights of ISL data within EQ preparation zone for 15 days before and 5 days after the Chile event to further confirm the TEC calculations.

The EQ preparation zone for the M7.7 Chile event was obtained by the formula proposed by Dobrovolsky et al (1979):

$$R = 10^{0.43M} \quad (4)$$

where M is the magnitude and R is the radius of the EQ preparation zone. Eq. (4) shows that the radius of EQ preparation zone is only dependent on the EQ magnitude, i.e. strong EQs may have large preparation zones and vice versa. In this paper, we averaged the DEMETER measurements for the orbits only occurred within the EQ preparation zone.

3. Observations and results

To interpret the ionospheric anomalies over the epicenter of the impending EQ in the southern Chile, GPS TEC was examined to confirm the anomalies within 18 days before and 2 days after the main

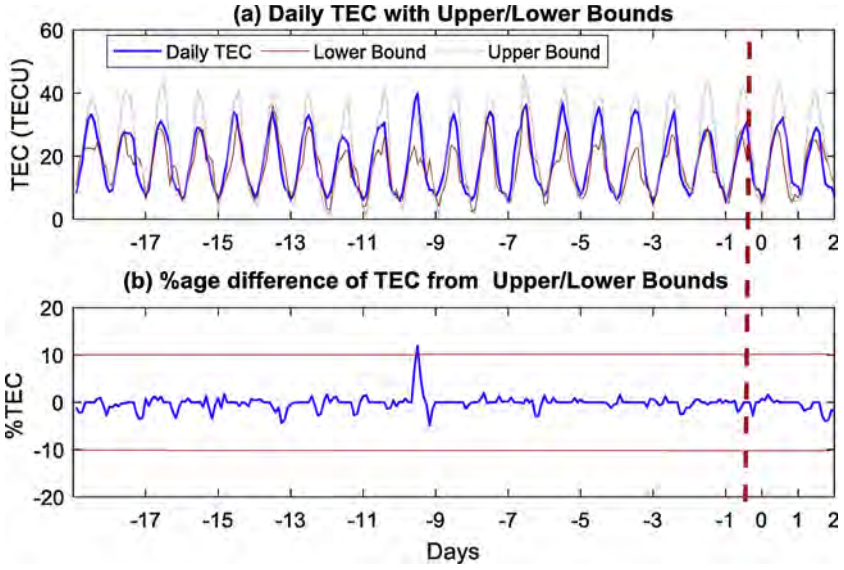

Fig. 3. The diurnal GPS TEC values before and after the Chile event bounded by the confidence intervals. The unit of TEC is 10^{16} el/m^2. The days are shown against the TEC values on y-axis. The EQ time is denoted by the red dashed line (For interpretation of the references to colour in this figure legend, the reader is referred to the web version of this article).

shock along with the confidence bounds (Fig. 3a). The daily TEC values with confidence bounds and percentage deviation are obtained over the epicenter from the measurements of dense GPS receivers. The daily TEC with bounds are plotted against the days of the year, represented by days before and after the event. Similarly, the percentage deviation of TEC showed significant perturbation on 9 days before the main shock of the M7.7 EQ (Fig. 3b). It is obtained by the difference of the original TEC values and upper/lower confidence bound (i.e., $TEC_{original} - TEC_{upper/lower\ bounds}$). After correlating the TEC with the global geomagnetic storm conditions, it is clear that the enhancement in TEC on the day (-9) may be due to the EQ (i.e., this enhancement occurred during the period of quiet storm days).

The daily temporal TEC against the days in Fig. 3b shows a significant deviation from the rest of the data before the EQ day, where the main shock day is marked by a red dotted line in both the panels. The abnormality detected was then measured by the percentage deviation method, which is more than 10% of the measured TEC from the confidence interval of mean and standard deviation. To measure this variation of electron contents spatially, the differential TEC maps are investigated for the suspected day of November 05, 2007 (i.e. 9 days before the EQ day), as shown in Fig. 4, Panel b. Furthermore, the TEC maps over the epicenter are also analyzed for November 04, 2007 (Fig. 4; Panel a) and November 06, 2007 (Fig. 4; Panel c). For this Figure, the monthly mean TEC is extracted from the TEC map of the observed day for specific UT hour ($dTEC_{UT} = TEC_{daily,\ UT} - TEC_{monthly,\ UT}$). The purpose of illustrating the TEC maps is to verify the execution of seismic perturbations in the ionosphere with in situ measurements on the suspected day and further clarify that whether these anomalies are localized to the epicenter or not. The presence of abnormal TEC clouds over the epicenter on November 05, 2007 and the absence on November 04 and 06, 2007 showed that these electron clouds is not a global feature, which may result due to solar or magnetic storms, but it is certainly associated to the EQ.

Interestingly, TEC variations are noticed over the epicenter from UT = 16:00 to UT = 20:00 during the EQ preparation period on November 5, 2007 (i.e. 9 days before the EQ day) as presented in Fig. 4b. However, the analysis of the TEC maps during UT 16:00-18:00 on November 04 and 06, 2007 showed no EQ perturbations before the main shock within the seismogenic zone. The purpose of analyzing the TEC maps on three consecutive days (i.e. November, 04, 05 and 06, 2007) is to check whether the variation is related to EQ or not. However, the abnormal clouds confirmed the existence of TEC variation with the EQ epicenter on November 05, 2007. Which is then followed by the EQ main shock on November 14, 2007, at UT = 15:40. The TEC anomalies on November 05, 2007, during UT = 16:00 to UT = 20:00 are not coincident. However, it is a clue about the EQ precursors. It shows that EQ precursors can be seen during the same UT hours (or local time) as the main shock. However, it needs more statistical analysis on the past EQs by estimating the TEC over the epicenters. Another important aspect of TEC clouds is the eastward drift, which could be due to the plasma flow from the epicenter to the ionosphere (Kuo et al., 2011; Ryu et al., 2014). Following the previous findings, the eastward drift in this study is more intensified in the spatial map during UT = 16:00- 20:00 on November 05, 2007, which may be due to the plasma shift from the compression of rocks in the EQ prone region.

However, to confirm the ionospheric perturbations, we extended our analysis for the real precursor by studying the ascending orbits data of electron density and electron temperature from DEMETER satellite. The measurements of DEMETER retrieved from the orbits of the satellite occurred within the EQ preparation zone are plotted against the days (Fig. 5). These measurements include the electron density and electron temperature over the epicenter of the future event. As discussed earlier, DEMETER was launched in sun-synchronous orbit at 710 km altitude with ascending node crossing the local equatorial part at 22:00 LT (nighttime) and 10:30 LT (daytime). Therefore, all the measurements were retrieved at 710 km over the epicenter during daytime from the ascending mode of the satellite orbits. The temporal electron density from DEMETER showed enhancement beyond the upper confidence interval on nine days before the event in accordance with the TEC measurements. However, the electron temperature showed depletion on days (-9, -8 and -7) related to the EQ. The upper and lower confidence bounds are obtained from the median and standard deviation ($\mu \pm 2\sigma$) of 15 days before and 5 days after the event, as shown in both panels of Fig. 5. The anomalous value in DEMETER ISL measurements is the day (-9), where the enhancement and depletion are more probable than the other values. On the contrary, DEMETER ascending orbits measurements show no perturbations on November 12 and 13, 2007 related to the geomagnetic storm, where the Kp values are greater than three during these days. The analysis of DEMETER measurements confirmed that pre seismic ionospheric anomalies are more significant than post seismic anomalies. On the other hand, anomalies related to geomagnetic is not prominent in the DEMETER data. Therefore the enhancement in temporal electron density and depletion in electron temperature are most probably related to the M7.7 event.

To provide a stringent proof to the temporal ionospheric anomalies, the spatial maps of electron density and electron temperature from DEMETER ascending orbits are studied over the epicenter by the Diffusion interpolation with barriers in ArcGIS software. For this study, we interpolated the electron density and electron temperature from

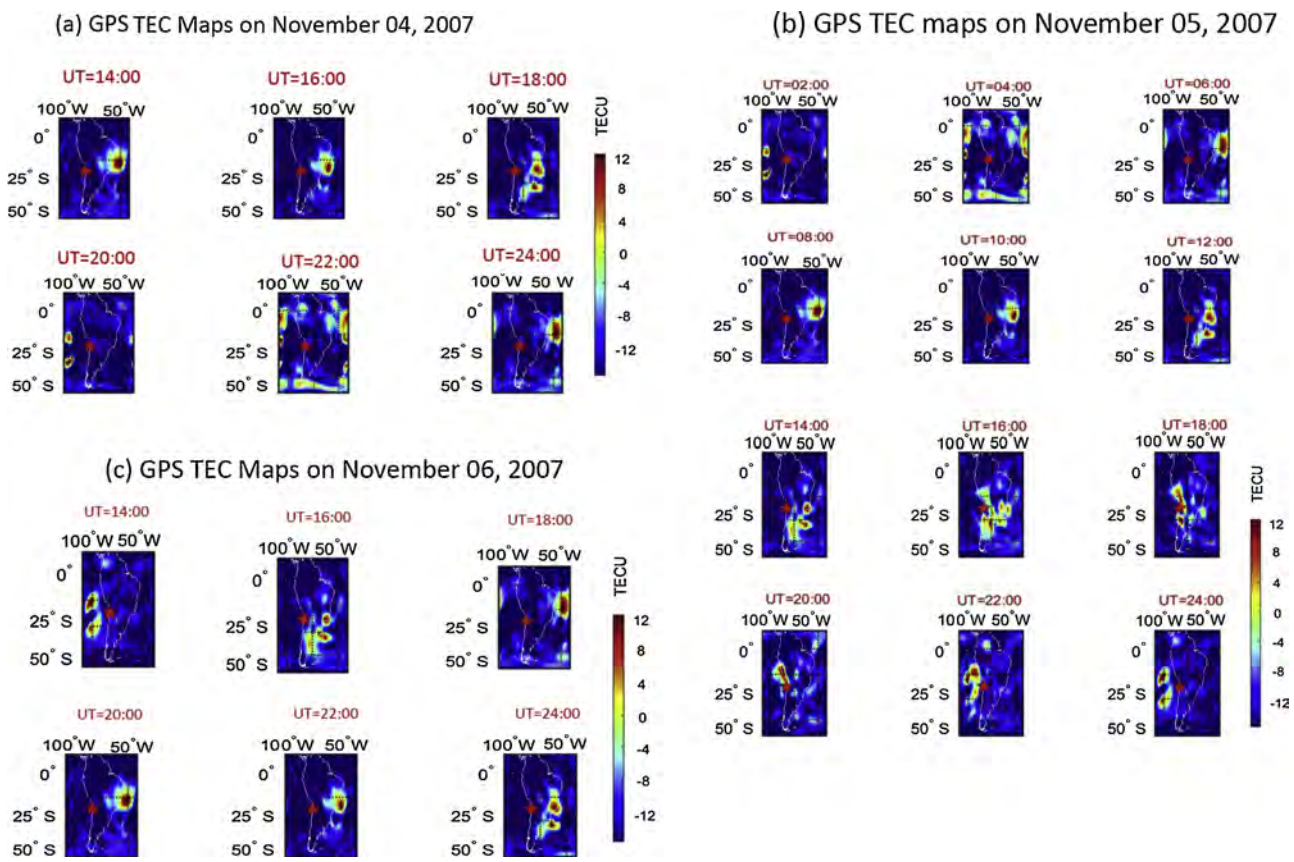

Fig. 4. Spatial TEC maps over the epicenter of M7.7 Chile EQ (a) November 04, 2007, (b) November 05, 2007 and (c) November 06, 2007. The red filled star is the epicenter of the EQ; however, the legend bar with TECU is the unit of TEC deviation during each UT hours (For interpretation of the references to colour in this figure legend, the reader is referred to the web version of this article).

ascending flight during November 03-06, 2007 (Figs. 6 & 7). The enhancement on November 05, 2007, in the electron density is prominent over the epicenter from the rest, which is probably the propagation of plasma flow in the upper ionosphere. Similarly, the prompt depletion in electron temperature on November 05, 2007 is also significant over the epicenter from the ascending orbits of DEMETER (Fig. 7). The variation in data was shown in the same unit as the original unit of the electron density and temperature; however it was calculated from the interpolation of each profile. The low electron temperature values over the EQ preparation zone in the spatial value exhibit the significant deviation, which is also prominent in the temporal analysis of the averaged electron temperature.

To further confirm the asymmetry between the upper and lower limbs of electron density and electron temperature along latitude around the epicenter within the EQ preparation zone, the Index number (No.) was calculated. As the EQ preparation zone extends from 0 °S to

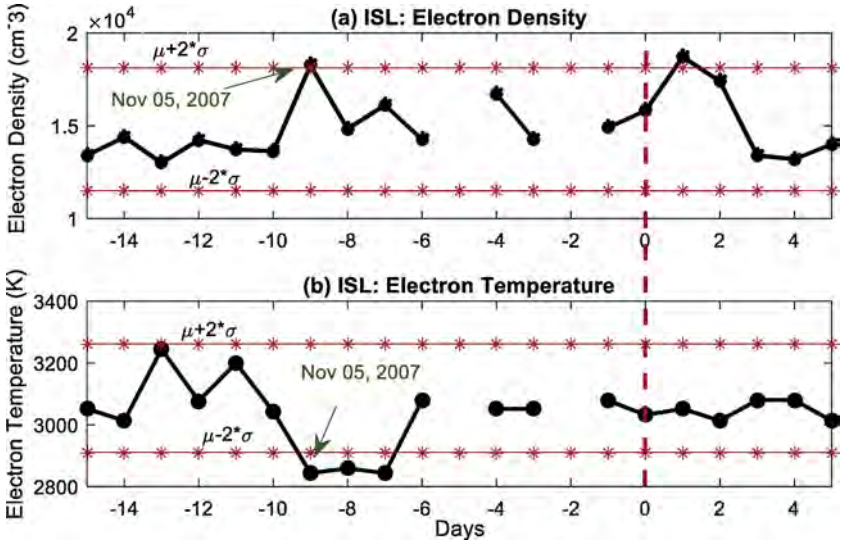

Fig. 5. The averaged ISL (Langmuir probe) measurements from DEMETER satellite above the epicenter of the EQ. (a) The electron density along with the confidence bounds in the context of the M7.7 EQ. (b) The electron temperature against the days along X-axis before and after the main shock. The 0 indicates the EQ day.

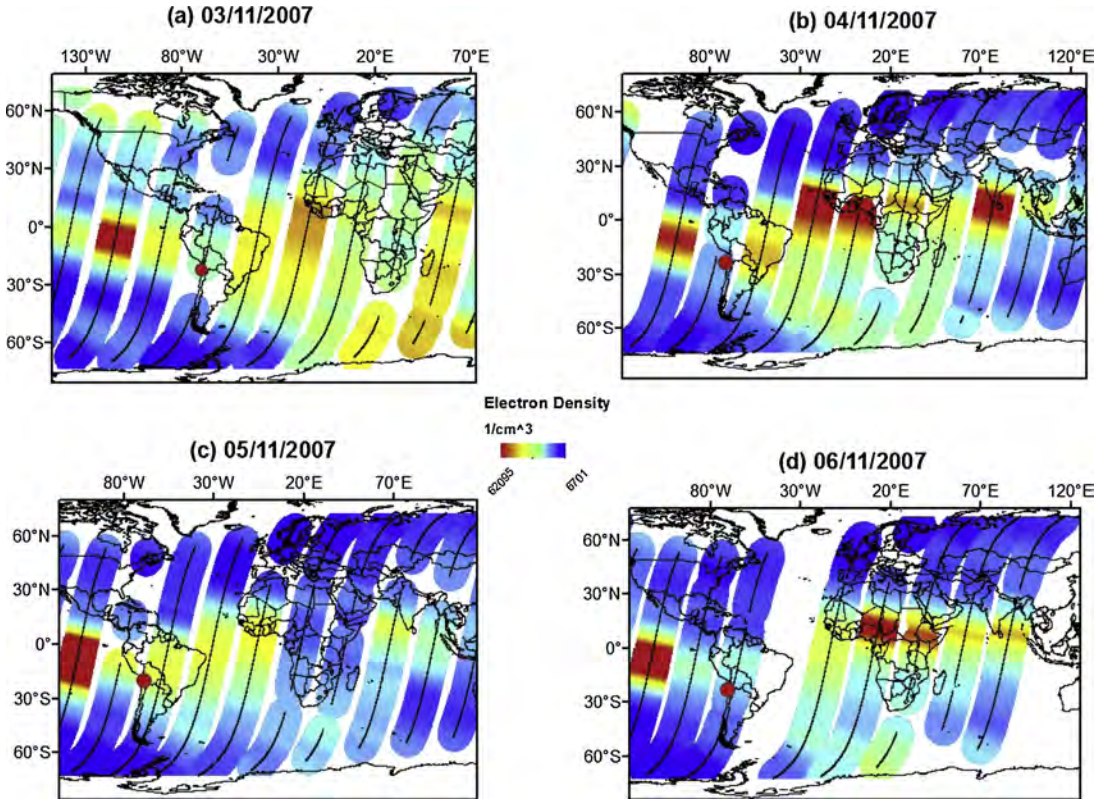

Fig. 6. The interpolation of the electron density for the DEMETER daytime observations. The epicenter is represented by red star in circle while the legends show the variation in electron density. The half orbits of DEMETER are shown by black lines (For interpretation of the references to colour in this figure legend, the reader is referred to the web version of this article).

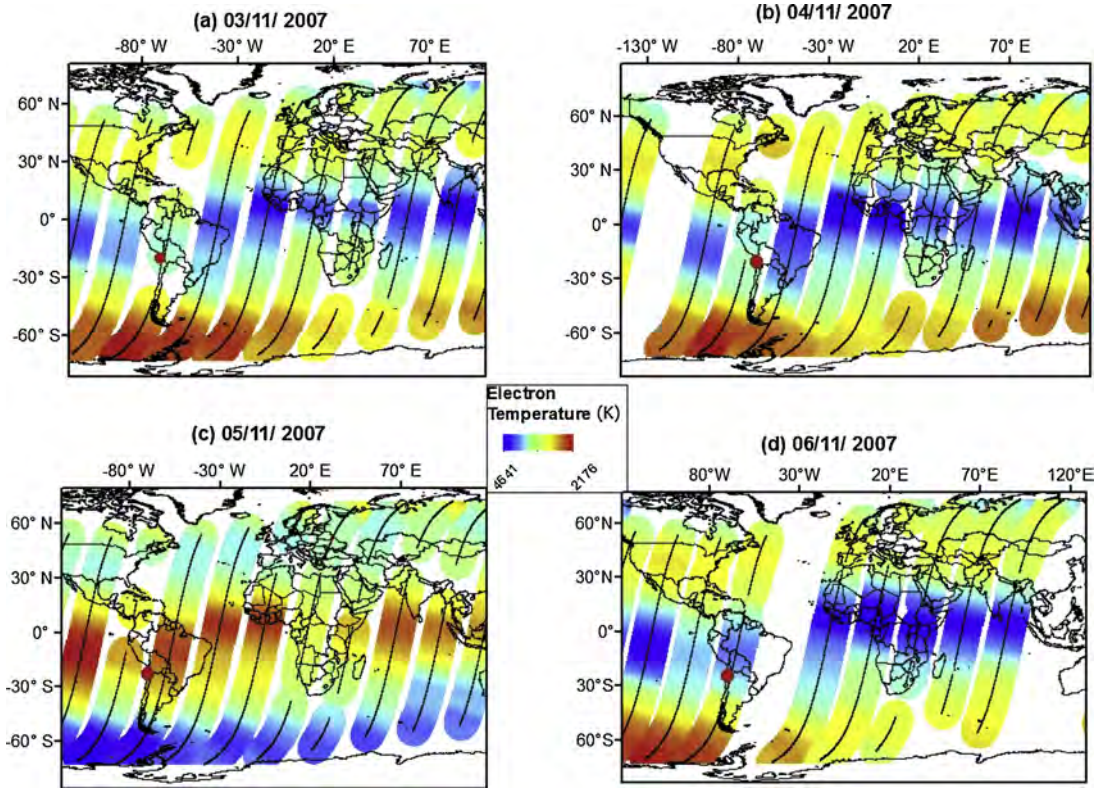

Fig. 7. The interpolation of the electron temperature from the DEMETER ISL daytime observations around the epicenter of M7.7. The days and legend are clearly shown for the suspected days. The red filled circle is the epicenter, while the black lines are the DEMETER half orbits (For interpretation of the references to colour in this figure legend, the reader is referred to the web version of this article).

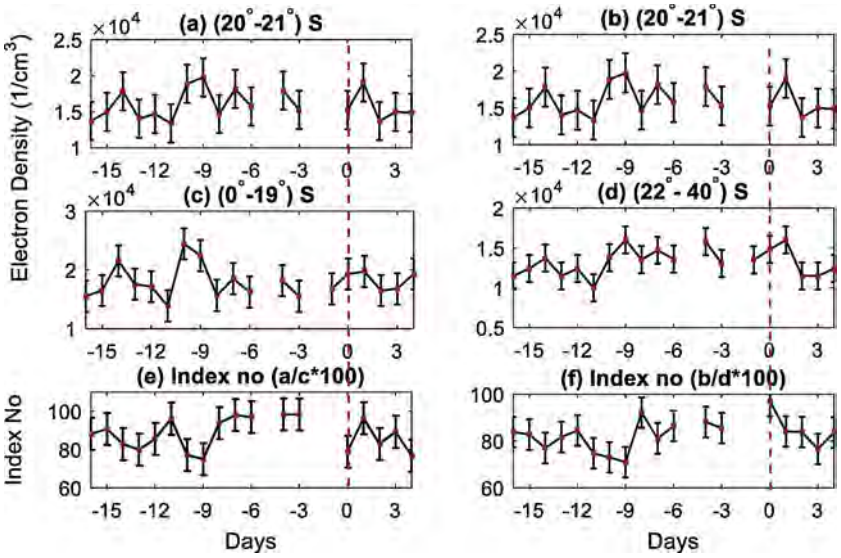

Fig. 8. (a-b) The DEMETER electron density values on the EQ latitude (20 ˚S-21 ˚S) for 16 days before and 4 days after the main-shock. (c-d) Similarly, the measurements of DEMETER for the northern and southern sectors around the epicenter along the latitude within the EQ preparation zone. (e-f) the Index No. obtained for both the direction around the epicenter latitude of the M7.7 EQ.

42 ˚S around the epicenter along latitude, the daily measurements from DEMETER ISL for all the flights are used for analysis. The Index No. is calculated by;

$$Index\ No = \frac{P_o}{P_{N/S}} \times 100 \tag{5}$$

Where P_o is the averaged DEMETER measurement at (20-21) ˚ S (i.e. epicenter latitude) and $P_{N/S}$ is the averaged ISL measurements for the northern and southern sectors around the epicenter. The electron density and electron temperature measurements for the northern sector above the epicenter are averaged from 0 ˚S to 19 ˚S along the latitude within the EQ preparation zone. However, for the southern side of the epicenter, the measurements are averaged from 22 ˚S to 42 ˚S.

The Index No. of electron density for the epicenter latitude and north side of the epicenter showed the abrupt variation on November 05, 2007, which is abnormal from the rest of the values (Fig. 8; Panel a & c). Similarly, the Index No. for the southern side also behaved abnormally like the northern sector of the electron density within the EQ preparation zone (Fig. 8 Panel b & d). All the abnormal values showed a correlation with the daily averaged DEMETER measurements bounded by the confidence intervals. Similarly, it also showed abnormality in accordance with the TEC values, which drove to the conclusion of immense energy flow from the EQ preparation zone to the ionosphere.

The Index No. for the electron temperature on the northern and southern side of the epicenter within the EQ preparation zone showed a decline from the rest of the days before the event (Fig. 9). The northern side electron temperature having Index No. 70% (see e.g. Fig. 9; Panel, a & c), while that of the southern side is 65% (e.g. Fig. 9; Panel, b & d).

Furthermore, the mutual study of the electron density and electron from DEMETER at EQ latitude and its conjugate axis (i.e (20˚-21 ˚S) and (20˚-21 ˚N)) showed a clear deviation over the EQ epicenter latitude (Fig. 10). For this purpose, the ISL electron density and electron temperature are averaged over the EQ latitude sector and its conjugate axis. The variation on November 05, 2007 in electron density and electron temperature is prominent from rest of the days at EQ latitude than the conjugate axis. It means that the deviations in DEMETER measurements over the EQ sector are due to the future event.

4. Discussion

In this paper, the ionospheric anomalies from GPS TEC and DEMETER satellite (electron density and electron temperature) is studied before and after the M7.7 Chile EQ (November 14, 2007) that hits the south of Chile. The ionospheric data including TEC and electron (density and temperature) of DEMETER showed clear abnormalities over the epicenter before the main shock day during quiet geomagnetic storm. We found evidence of deviation (more than 10% of the observed values) beyond the statistical bounds on November 05, 2007 (9 days before the main shock) in GPS TEC measurements within the seismogenic zone around the epicenter of the impending EQ.

The temporal TEC values over the epicenter in Fig. 3a showed significant variations on November 05, 2007 (9 days before the EQ), which is more than 10 % from the normal distribution in the percentage deviation analysis (Fig. 3b). The temporal plot provides significant information about the suspected seismo ionospheric day; however, it illustrated no information about the suspected hours. For this purpose, the spatial maps of TEC for November 04-06, 2007 over the epicenter of M7.7 EQ are retrieved to further monitor the abnormal UT hours related to the main shock. Interestingly, it is found that the epicenter is covered by thick TEC clouds on November 05, 2007 during UT˜16:00-20:00 with the seismogenic zone (Fig. 4b). Similarly, the TEC maps for November 04, 2007 (Fig. 4a) and November 06, 2007 (Fig. 4c) are also analyzed over the epicenter for the confirmation of abnormal ionospheric clouds during UT˜16:00-20:00 on the suspected day. After careful observations of the TEC maps on three consecutive days (i.e. November, 04-06, 2007), it is confirmed that unusual ionospheric clouds on November 05, 2007 during UT˜16:00-20:00 is probably related to the main shock of the impending EQ. This study found critical evidence of reasonable ionospheric anomalies 9 days before the EQ day of M7.7, Chile. On the contrary, Liu et al. (2004) found a remarkable correlation between ionospheric TEC derived from ground-based receiver of GPS and M ≥ 6.0 EQs within 5 days before the event (16 out of the 20 large quakes). The correlation of seismo ionospheric anomalies with EQs in Liu et al. (2004) and this study show that both the reduction and enhancement in the ionosphere are associated to the EQ induced electric field from beneath. However, the propagation of pre seismic ionospheric anomalies as a result of electric filed generation before the EQ during the preparation period over the epicenter is proposed by Kuo et al. (2011).

The evolution and propagation of pre-seismic TEC anomalies in the ionosphere is not yet understood by the current analysis. However, Shklyar and Truhlík (1998) pointed out the direction of the field and initial condition of the electron density distribution, reduced effect of the particle density in the region of field localization over the epicenter of the future EQ. Similarly, Kuo et al. (2011) presented the stressed-rock in the EQ regions as the source of the electric field at the lower end of the ionosphere. In their case, the numerical simulations showed significant anomalies in the ionosphere over the seismogenic zones after

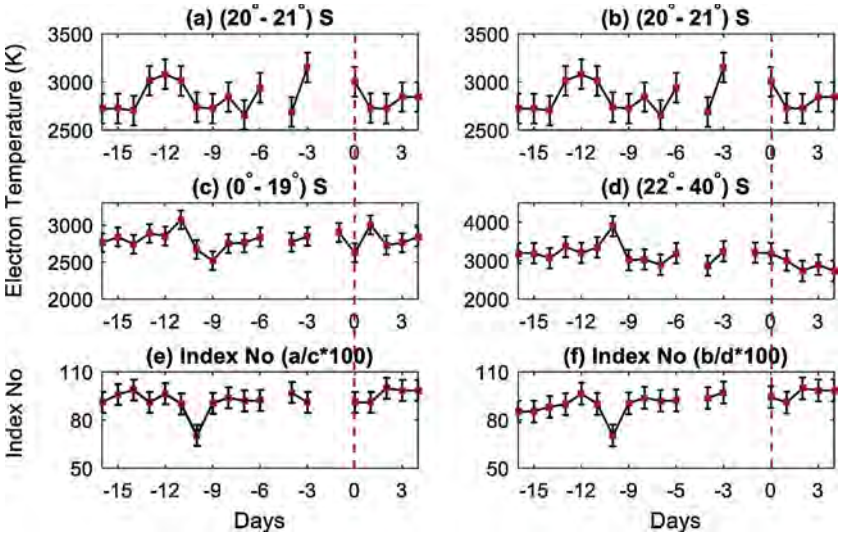

Fig. 9. (a-b) The DEMETER electron temperature measurements over the EQ latitude (20 °S-21 °S) for 16 days before and 4 days after the main-shock. (c-d) Similarly, the measurements of DEMETER for the northern and southern sectors around the epicenter along the latitude within the EQ preparation zone. (e-f) the Index No. obtained for both the direction around the epicenter latitude of the M7.7 EQ. The EQ day is denoted by a red dotted line (For interpretation of the references to colour in this figure legend, the reader is referred to the web version of this article).

the execution of the electric field. They further showed the same increment and depletion in TEC and concluded the deviation of TEC due to the occurrence of huge mega-thrust. The simulated results in Figs. () in Kuo et al. (2011) showed the dense clouds of ionospheric electron density and electron temperature, and plasma movement on meridian planes over the epicenter of future EQ. Furthermore, they showed that the global disruption of the ionosphere could be due to the electric field generated at the epicenter, accumulated in the form of hole-charge carriers near the Earth's surface. Their simulation results support the observed anomalies in our case study that the seismic plasma sink and plasma fountain effect also exist in the direction of the electric field in the atmosphere over the seismic breeding zone. The direction of the plasma shift caused by the E × B drift around the EQ epicenter is the same on both sides of the magnetic equator. In other words, the upwards (downwards) motion of the plasma drift around the epicenter caused the plasma to move upwards (downwards) in the magnetic conjugate regions.

In this paper, we also analyzed the day time DEMETER satellite data for 15 days before and 5 days after the main shock day within the seismogenic zone around the epicenter, as estimated by Dobrovolsky et al. (1979). We found a significant enhancement above the upper confidence bound in the temporal estimation of electron density on November 05, 2007 (Fig. 5a) and similarly a depletion in electron temperature is also recorded on the same day before the main shock (Fig. 5b). One can see these prominent ionospheric perturbations in the measurements of GPS TEC, which is another strong evidence of multi-precursors ionospheric anomalies before the Chile event. The spatial maps of DEMETER ascending orbits during November 03-06, 2007 confirmed the anomalous enhancement in electron density (Fig. 6) and similarly depletion in electron temperature from ISL measurement over the epicenter (Fig. 7). The pre-seismic ionospheric anomalies in the measurements of DEMETER satellite can be portrayed in the light of previous reports on satellite based ionospheric precursors. Previously, Oyama et al. (2011) reported the cause of reduction in the ion density data (measured from the DE-2 satellite) related with a mighty EQ (latitude: -33.13°, longitude: 73.07°, M7.5, October 1981) to the plasma drift induced perpendicular to the magnetic field of the earth. The plasma drift (attributed as 'the seismic plasma fountain effect') in Oyama et al. (2011) was explained as the end product of the ionospheric dynamo electric field that raised the plasma to a certain altitude over the quake region. Another such example of ionospheric depletion prior and after large magnitude EQs was also published by Oyama et al.

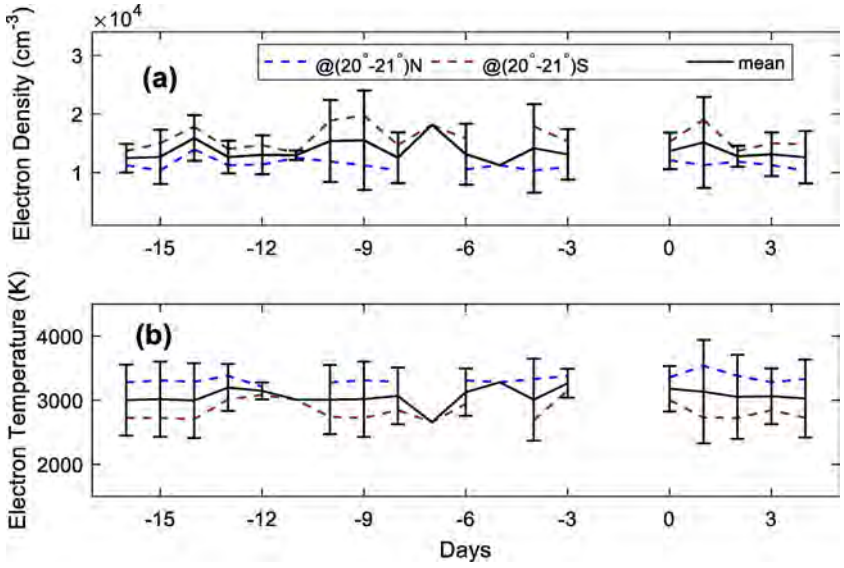

Fig. 10. The symmtary between the EQ latitud and its conjugate in the measurements of electron density and electron temperature from DEMETER satellite. It is clear that the variation on November 5, 2007 (9 days before the event) at epeicenter latitude flutuates more than the measurements at conjugate axis.

(2008). In that paper, Oyama et al. (2008) observed the significant reduction in the ionospheric data of the HINOTORI satellite during three EQs in late 1981 and early 1982 in the Philippines, which were due to the generation of a westward electric field over the epicenter. However, they pointed that the afternoon period of the electron density data significantly reduced over the magnetic conjugate point; by contrast, we observed an enhancement in electron density over the epicenter (Fig. 5a). On the other hand, we observed an anomalous reduction in electron temperature within ten days prior to the event (Fig. 5a). Ruzhin et al. (1998) found the EQ induced very low frequency (VLF) and F2-peak parameters anomalies on magnetically conjugated regions in the observation of INTERCOSMOS-18 and ALOUETTE satellites. The robust electro-dynamic coupling in the ionosphere on the two sides of the geomagnetic field is the consequence of the immense conducting along the geomagnetic tube lines. Interestingly, the previously known wave phenomena in the upper ionosphere was reported as the magnetospheric processes rather than attributing to the seismic induced ionospheric precursors (Onishi et al., 2011).

This paper also includes further analysis on the asymmetry of electron density and electron temperature on the EQ epicenter and its conjugate axis (Figs. 8–10). Interestingly, these results imply a significant perturbation over the EQ epicenter as compared to the conjugate axis, as represented by the Index No (Figs. 8 & 9). The reason of these anomalies in DEMETER measurements is the exchange of energy between the lithosphere and ionosphere by the EQ during the preparation period before the main shock day (Ryu et al., 2014). Similar coupling of DEMETER based electron density and worldwide seismic events during the DEMETER mission is reported statistically by Li and Parrot (2012). They conducted a statistical study for the global $M \geq 4.8$ EQs occurred during the period of DEMETER mission i.e. from July 2004 to December 2010. The increment in the electron density for the studied EQs mostly increased with the rise in the magnitude of the EQ. They found that 88% of the anomalies in the electron density were related to EQs in the DEMETER data.

The significant anomalies that appeared in the ionospheric parameters measured by GPS TEC and DEMETER around the main shock are distinguished to be due to changes in the initial conditions, if the anomalies are assumed to be raised due to the seismo ionospheric fountain (sink) model (Kuo et al., 2011). The eastward (or westward) electric fields produce the upward (or downward) plasma movement, according to the alignment of the $E \times B$ drift geometry and geomagnetic field line. Namgaladze et al. (2009) pointed out that the upward plasma motion transfers significant electron drift in the F2 layer of the atmosphere because of reduction of dominating O^+ ions in the ion-molecular reaction in the mid-latitude region. In this paper, the enhanced plasma density implies that the significant anomalies in the ionosphere were probably occurred by the upward drift of the plasma around seismogenic zones. However, with the existing equipment of ground and satellite-based ionospheric observations, more dedicated missions are required to properly detect the right ionospheric precursor associated with EQ.

5. Conclusion

The ionospheric anomalies associated with the M7.7 Chile EQ of November 14, 2007, were investigated using the total electron content data from the global GPS network, in addition to the spatial and temporal electron density and temperature from the DEMETER satellite. In the daily temporal ionospheric parameters, significant deviation of the electron density was observed before the main shock (i.e. November 05, 2007) in the GPS TEC data, and subsequently in the DEMETER analyses. While previous reports have confirmed the enhancement in TEC few days before the event during quiet geomagnetic storm, this study revealed that the enhancement was part of the plasma shift in the dayside from the epicenter to the ionosphere within 9 days (on November 05, 2007) before the main shock and the intensity lasts immediately after the event. The asymmetry in electron density and temperature of DEMETER measurement over the EQ epicenter and its conjugate axis showed ionospheric deviation between lithosphere and ionosphere over the epicenter of M7.7, Chile event during the EQ preparation period. Furthermore, the spatial maps of electron density and temperature from DEMETER on the confirmed abnormal clouds over the EQ epicenter of the future EQ on November 5, 2007. The anomalies in the electron density and electron temperature during the dayside and the parallel enhancements in the TEC support that these anomalies may be due to the induction of EQ over the seismogenic zone.

Acknowledgement

The authors are very grateful to the IGS community for providing the GIM-TEC data. We are also very thankful to the USGS, OMNI web and Kyoto University for providing EQ and geomagnetic storm data, respectively. Further thanks to the administration of DEMETER satellite for open access data.

References

Arslan, M., Shah, M., Hernández-P, M., Iqbal, T., 2019. Pre-earthquake ionospheric anomalies before three major earthquakes by GPS-TEC and GIM-TEC data during 2015-2017. Adv. Space Res. https://doi.org/10.1016/j.asr.2018.12.028.

Altadill, D., Apostolov, E.M., 2003. Time and scale size of planetary wave signatures in the ionospheric F region: Role of the geomagnetic activity and mesosphere/lower thermosphere winds. J. Geophys. Res.: Space Phys. 108 (A11) p. n/a-n/a.

Berthelier, J.J., Godefroy, M., Leblanc, F., Malingre, M., Menvielle, M., Lagoutte, D., Brochot, J.Y., Colin, F., Elie, F., Legendre, C., Zamora, P., Benoist, D., Chapuis, Y., Artru, J., Pfaff, R., 2006. ICE, the electric field experiment on DEMETER. Planetary Space Sci. 54 (5), 456–471. https://doi.org/10.1016/j.pss.2005.10.017.

Bošková, J., Šmilauer, J., Jiříček, F., Tříska, P., 1993. Is the ion composition of the outer ionosphere related to seismic activity? J. Atmosph. Terrestrial Phys. 55 (13), 1689–1695. https://doi.org/10.1016/0021-9169(93)90173-V.

Chmyrev, V.M., Isaev, N.V., Serebryakova, O.N., Sorokin, V.M., Sobolev, Y.P., 1997. Small-scale plasma inhomogeneities and correlated ELF emissions in the ionosphere over an earthquake region. J. Atmosph. Solar-Terrest. Phys. 59 (9), 967–974. https://doi.org/10.1016/S1364-6826(96)00110-1.

Cussac, T., Clair, M.-A., Ultré-Guerard, P., Buisson, F., Lassalle-Balier, G., Ledu, M., Elisabelar, C., Passot, X., Rey, N., 2006. The Demeter microsatellite and ground segment. Planetary Space Sci. 54 (5), 413–427. https://doi.org/10.1016/j.pss.2005.10.013.

Dobrovolsky, I.R., Zubkov, S.I., Myachkin, V.I., 1979. Estimation of the size of earthquake preparation zones. Pure Appl. Geophys. 117, 1025–1044. https://doi.org/10.1007/BF00876083.

Freund, F., 2002. Charge generation and propagation in igneous rocks. J. Geodyn. 33 (4), 543–570. https://doi.org/10.1016/S0264-3707(02)00015-7.

Fujiwara, H., Kamogawa, M., Ikeda, M., Liu, J.Y., Sakata, H., Chen, Y.I., Ofuruton, H., Muramatsu, S., Chuo, Y.J., Ohtsuki, Y.H., 2004. Atmospheric anomalies observed during earthquake occurrences. Geophys. Res. Lett. 31 (17). https://doi.org/10.1029/2004GL019865.

Geller, R.J., Jackson, D.D., Kagan, Y.Y., Mulargia, F., 1997. Earthquakes cannot be predicted. Science 275 (5306). https://doi.org/10.1126/science.275.5306.1616. p. 1616-1616.

Gokhberg, M.B., Gufeld, I.L., Rozhnoy, A.A., Marenko, V.F., Yampolsky, V.S., Ponomarev, E.A., 1989. Study of seismic influence on the ionosphere by super long-wave probing of the Earth-ionosphere waveguide. Phys. Earth Planetary Inter. 57 (1), 64–67. https://doi.org/10.1016/0031-9201(89)90214-8.

Gusman, A.R., Murotani, S., Satake, K., Heidarzadeh, M., Gunawan, E., Watada, S., Schurr, B., 2015. Fault slip distribution of the 2014 Iquique, Chile, earthquake estimated from ocean-wide tsunami waveforms and GPS data. Geophys. Res. Lett. 42 (4), 1053–1060. https://doi.org/10.1002/2014GL062604.

Hayakawa, M., Tomizawa, I., Ohta, K., Shimakura, S., Fujinawa, Y., Takahashi, K., Yoshino, T., 1993. Direction finding of precursory radio emissions associated with earthquakes: a proposal. Phys. Earth Planet. Interiors 77 (1), 127–135. https://doi.org/10.1016/0031-9201(93)90038-B.

Heki, K., Enomoto, Y., 2013. Preseismic ionospheric electron enhancements revisited. J. Geophys. Res.: Space Phys. 118, 6618–6626. https://doi.org/10.1002/jgra.50578.

Ho, Y.Y., Liu, J.Y., Parrot, M., Pinçon, J.L., 2013. Temporal and spatial analyses on seismo-electric anomalies associated with the 27 February 2010 M = 8.8 Chile earthquake observed by DEMETER satellite. Nat. Hazards Earth Syst. Sci. 13 (12), 3281–3289. https://doi.org/10.5194/nhess-13-3281-2013.

Junaid, A., Shah, M., Waqar, A.Z., Muhammad, A.A., Iqbal, T., 2018. Seismoionospheric anomalies associated with earthquakes from the analysis of the ionosonde data. J. Atmosph. Solar-Terrestrial Phys. 179, 450–458. https://doi.org/10.1016/j.jastp.2018.10.004.

Kuo, C.L., Huba, J.D., Joyce, G., Lee, L.C., 2011. Ionosphere plasma bubbles and density variations induced by pre-earthquake rock currents and associated surface charges. J. Geophys. Res.: Space Phys. 116. https://doi.org/10.1029/ 2011JA016628.

Larkina, V.I., Migulin, V.V., Molchanov, O.A., Kharkov, I.P., Inchin, A.S., Schvetcova, V.B., 1989. Some statistical results on very low frequency radiowave emissions in the upper ionosphere over earthquake zones. Phys. Earth Planetary Inter. 57 (1), 100–109. https://doi.org/10.1016/0031-9201(89)90219-7.

Li, M., Parrot, M., 2012. "Real time analysis" of the ion density measured by the satellite DEMETER in relation with the seismic activity. Nat. Hazards Earth Syst. Sci. 12 (9), 2957–2963. https://doi.org/10.5194/nhess-12-2957-2012.

Liu, J.Y., Chuo, Y.J., Shan, S.J., Tsai, Y.B., Chen, Y.I., Pulinets, S.A., Yu, S.B., 2004. Pre-earthquake ionospheric anomalies registered by continuous GPS TEC measurements. Ann. Geophys. 22 (5), 1585–1593. https://doi.org/10.1029/2008JA013698.

Liu, J.Y., Chen, Y.I., Chuo, Y.J., Chen, C.S., 2006. A statistical investigation of pre-earthquake ionospheric anomaly. J. Geophys. Res.: Space Phys. 111. https://doi.org/10.1029/2005JA011333.

Namgaladze, A.A., Klimenko, M.V., Klimenko, V.V., Zakharenkova, I.E., 2009. Physical mechanism and mathematical modeling of earthquake ionospheric precursors registered in total electron content. Geomagnet. Aeron. 49 (2), 252–262. https://doi.org/10.1134/S0016793209020169.

Ondoh, T., 2003. Anomalous sporadic-E layers observed before M 7.2 Hog-ken Abu earthquake; Terrestrial gas emanation model. Adv. Polar Upper Atmos. Res (17), 96–108.

Oyama, K.-I., Kakinami, Y., Liu, J.-Y., Kamogawa, M., Kodama, T., 2008. Reduction of electron temperature in low-latitude ionosphere at 600 km before and after large earthquakes. J. Geophys. Res.: Space Phys. 113. https://doi.org/10.1029/2008JA013367.

Oyama, K.I., Kakinami, Y., Liu, J.Y., Abdu, M.A., Cheng, C.Z., 2011. Latitudinal distribution of anomalous ion density as a precursor of a large earthquake. J. Geophys. Res.: Space Phys. 116. https://doi.org/10.1029/2010JA015948.

Parrot, M., 2002. The micro-satellite DEMETER. J. Geodyn. 33 (4), 535–541. https://doi.org/10.1016/S0264-3707(02)00014-5.

Parrot, M., Berthelier, J.J., Lebreton, J.P., Sauvaud, J.A., Santolik, O., Blecki, J., 2006. Examples of unusual ionospheric observations made by the DEMETER satellite over seismic regions. Phys. Chem. Earth Parts A/B/C 31 (4–9), 486–495. https://doi.org/10.1016/j.pce.2006.02.011.

Parrot, M., 2009. Anomalous seismic phenomena: view from space. In: Hayakawa, M. (Ed.), Electromagnetic Phenomena Associated with Earthquakes. Transworld Research Network, Kerala, pp. 205–233.

Píša, D., Parrot, M., Santolík, O., 2011. Ionospheric density variations recorded before the 2010 Mw 8.8 earthquake in Chile. J. Geophys. Res.: Space Phys. 116. https://doi.org/10.1029/2011JA016611.

Rishbeth, H., 2007. Do earthquake precursors really exist? Eos Trans. Am. Geophys. Union 88 (29). https://doi.org/10.1029/2007EO290008. p. 296-296.

Ruzhin, Y.Y., Larkina, V.I., Depueva, A.K., 1998. Earthquake precursors in magnetically conjugated ionosphere regions. Adv. Space Res. 21 (3), 525–528. https://doi.org/10.1016/S0273-1177(97)00892-2.

Ryu, K., Parrot, M., Kim, S.G., Jeong, K.S., Chae, J.S., Pulinets, S., Oyama, K.I., 2014. Suspected seismo-ionospheric coupling observed by satellite measurements and GPS TEC related to the M7.9 Wenchuan earthquake of 12 May 2008. J. Geophys. Res.: Space Phys. 119 (12). https://doi.org/10.1002/2014JA020284. p.10,305-310,323.

Shah, M., Jin, S., 2015. Statistical characteristics of seismo-ionospheric GPS TEC disturbances prior to global Mw ≥ 5.0 earthquakes (1998–2014). J. Geodyn. 92, 42–49. https://doi.org/10.1016/j.jog.2015.10.002.

Shklyar, D.R., Truhlík, V., 1998. On the modification of light ion concentration profiles above seismically active regions : a qualitative consideration. J. Atmosph. Solar-Terrestrial Phys. 60 (10), 1025–1033. https://doi.org/10.1016/S1364-6826(98)00041-8.

Sorokin, V.M., Chmyrev, V.M., Isaev, N.V., 1998. A generation model of small-scale geomagnetic field-aligned plasma inhomogeneities in the ionosphere. J. Atmosph. Solar-Terrestrial Phys. 60 (13), 1331–1342. https://doi.org/10.1016/S1364-6826(98)00078-9.

Sorokin, V.M., Chmyrev, V.M., Yaschenko, A.K., 2003. Ionospheric generation mechanism of geomagnetic pulsations observed on the Earth's surface before earthquake. J. Atmosph. Solar-Terrestrial Phys. 65 (1), 21–29. https://doi.org/10.1016/S1364-6826(02)00082-2.

Survey, U.S.G., 2007b. M7.7 northern Chile, earthquake of 14 November 2007. ftp://hazards.cr.usgs.gov/maps/sigeqs/20071114/ 20071114.pdf (last accessed January 2008). .

Tronin, A.A., 1996. Satellite thermal survey—a new tool for the study of seismo active regions. Int. J. Remote Sens. (17), 1439–1455. https://doi.org/10.1080/01431169608948716.

Yagi, Y., Okuwaki, R., Enescu, B., Hirano, S., Yamagami, Y., Endo, S., Komoro, T., 2014. Rupture process of the 2014 Iquique Chile Earthquake in relation with the foreshock activity. Geophys. Res. Lett. 41 (12), 4201–4206. https://doi.org/10.1002/2014GL060274.

Zhang, X., Zeren, Z., Parrot, M., Battiston, R., Qian, J., Shen, X., 2011. ULF/ELF ionospheric electric field and plasma perturbations related to Chile earthquakes. Adv. Space Res. 47 (6), 991–1000. https://doi.org/10.1016/j.asr.2010.11.001.